Article

n-Type Field-Effect Transistors Made of an Individual Nitrogen-Doped Multiwalled Carbon Nanotube

Kai Xiao, Yunqi Liu, Ping'an Hu, Gui Yu, Yanming Sun, and Daoben Zhu

J. Am. Chem. Soc., **2005**, 127 (24), 8614-8617• DOI: 10.1021/ja042554y • Publication Date (Web): 27 May 2005

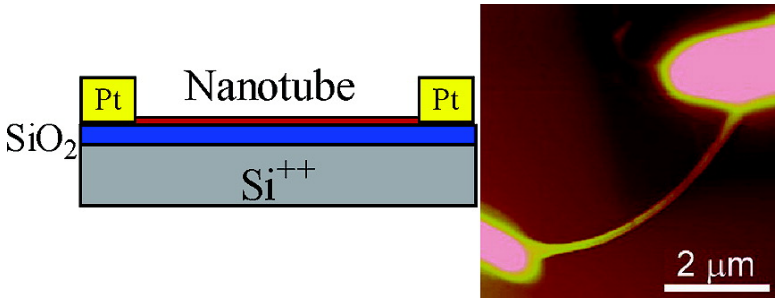

More About This Article

Additional resources and features associated with this article are available within the HTML version:

- Supporting Information
- Links to the 9 articles that cite this article, as of the time of this article download
- Access to high resolution figures
- Links to articles and content related to this article
- Copyright permission to reproduce figures and/or text from this article

View the Full Text HTML

J|A|C|S
ARTICLES
Published on Web 05/27/2005

n-Type Field-Effect Transistors Made of an Individual Nitrogen-Doped Multiwalled Carbon Nanotube

Kai Xiao,† Yunqi Liu,* Ping'an Hu, Gui Yu, Yanming Sun, and Daoben Zhu*

Contribution from the Key Laboratory of Organic Solids, Institute of Chemistry, Chinese Academy of Sciences, Beijing 100080, P. R. China

Received December 10, 2004; E-mail: liuyq@mail.iccas.ac.cn; zhudb@mail.iccas.ac.cn

Abstract: We report on the fabrication and characterization of field-effect transistor based on an individual multiwalled nitrogen-doped carbon nanotube. Our measurements show that the N-doped carbon nanotubes have n-type properties. The contact properties of the tube and Pt electrodes are also studied in detail. Temperature dependence of two-terminal transport experiments suggests that transport is dominated by thermionic emission and tunneling through a 0.2 eV Schottky contact barrier.

Introduction

In recent years, there has been much interest in the investigation of the electronic properties of carbon nanotubes (CNTs).[1] Theoretical work predicted that single-walled carbon nanotubes (SWCNTs) have semiconducting or metallic properties depending on their chirality,[2−4] suggesting SWCNTs and multiwalled carbon nanotubes (MWCNTs) as prime candidates for many applications in nanoelectronics. Thus, the control of the electronic properties of CNTs is of great technological importance; for example, doping them with other elements is a promising way to achieve this goal. Similar to conventional materials, doped nanotubes are expected to yield nanoscale devices with interesting properties and functions.[5−7] Lee et al. were the first to study the effect of doping on the conductivity of bulk samples of SWCNTs. Vapor-phase reaction with Br or K was found to increase electrical conductivity of SWCNTs up to a factor of 30 at room temperature.[8] These reactions suggest that the doping is carried out by intercalation, similar to graphite intercalation compounds. However, this is distinctively different from the substitutional doping, which is investigated in this article. Boron and/or nitrogen are two of the few elements that are expected to dope graphitic structures substitutionally and modify the electronic and structural properties.[9,10] Boron atoms contain one electron less compared with C; therefore, the electronic structure contains electronic holes, responsible for generating a p-type conductor. Wei et al.[11] measured the resistivity of an individual B-doped MWCNT and found reduced room-temperature resistance as compared with pure C nanotubes and, overall, semiconducting behavior. Semiconducting properties were also observed by Yu et al.[12] through photoluminescence spectra and by Golberg et al.[13] in a modified scanning tunneling microscopy on B−C−N compositions with a significant fraction of BN. Nitrogen atoms, similar to B atoms, can dope into carbon nanotube and change the electronic properties of the CNTs. The surface electronic structure of N-doped MWCNTs has been investigated using scanning tunneling spectroscopy, which revealed that the doped tubes have semimetallic properties with vanishing or narrow band gaps. The observation of two variants of the local density of states in different areas of the N-doped tubes suggested the segregation of the dopant into ordered NC_3 nanodomains.[14] Moreover, the temperature-dependent thermoelectric power of N-doped carbon nanotube mats has been measured, showing that such dopant can be used to modify the majority carrier conductivity.[15] Nitrogen, as a donor element, can strongly modify the electronic behavior and structure of CNTs. According to theoretical calculations, the nitrogen-containing pentagons can induce strong bending of the nanotubes and affect the alignment of the CNT lattice, resulting in the creation of donor states near the Fermi level. This is similar to the doping caused by "topological" defects, which result in the introduction of

† Present address: Center for Nanophase Materials Sciences, Oak Ridge National Laboratory, Oak Ridge, TN 37831.

(1) Bachtold, A.; Hadley, P.; Nakanishi, T.; Dekker, C. *Science* **2001**, *294*, 1317−1320.
(2) Mintmire, J. W.; Dunlap, B. I.; White, C. T. *Phys. Rev. Lett.* **1992**, *68*, 631−634.
(3) Hamada, N.; Sawada, S.; Oshiyama, A. *Phys. Rev. Lett*. **1992**, *68*, 1579−1581.
(4) Saito, R.; Fujita, M.; Dresselhaus, G.; Dresselhaus, M. S. *Phys. Rev. B* **1992**, *46*, 1804−1811.
(5) Esfarjant, K.; Farajian, A. A.; Hashi, Y.; Kawazoe, Y. *Appl. Phys. Lett*. **1999**, *74*, 79−81.
(6) Leonard, F.; Tersoff, J. *Phys. Rev. Lett.* **1999**, *83*, 5174−5177.
(7) Antonov, R. D.; Johnsom, A. T. *Phys. Rev. Lett*. **1999**, *83*, 3274−3276.
(8) Lee, R. S.; Kim, H. J.; Fischer, J. E.; Thess, A.; Smalley, R. E. *Nature (London*) **1997**, *388*, 255−257.
(9) Carroll, D. L.; Redlich, Ph.; Blasé, X.; Charlier, J. C.; Curran, S.; Ajayan, P. M.; Roth, S.; Ruhle, M. *Phys. Rev. Lett*. **1998**, *81*, 2332−2335.
(10) Terrones, H.; Terrones, M.; Hernández, E.; Grobert, N.; Charlier, J. C.; Ajayan, P. M. *Phys. Rev. Lett*. **2000**, *84*, 1716−1719.
(11) Wei, B.; Spolenak, R.; Kohler-Redlich, P.; Ruhle, M.; Arzt, E. *Appl. Phys. Lett*. **1999**, *74*, 3149−3151.
(12) Yu, J.; Ahn. J.; Yoon, S. F.; Zhang, Q.; Gan, B.; Chew, K.; Yu, M. B.; Bai, X. D.; Wang, E. G. *Appl. Phys. Lett.* **2000**, *77*, 1949−1951.
(13) Golberg, D.; Dorozhkin, P.; Bando, Y.; Dong, Z. C. *Chem. Phys. Lett.* **2002**, *359*, 220−228.
(14) Czerw, R.; Terrones, M.; Charlier, J. C.; Blasé, X.; Foley, B.; Kamalakaran, R.; Grobert, N.; Terrones, H.; Ajayan, P. M.; Blau, W.; Tekleab, D.; Ruhle, M.; Carroll, D. L. *Nano. Lett*. **2001**, *1*, 457−460.
(15) Choi, Y. M.; Lee, D. S.; Czerw, R.; Chiu, P. M.; Grobert, N.; Terrones, M.; Reyes-Reyes, M.; Terrones, H.; Charlier, J. C.; Ajayan, P. M.; Roth, S.; Carroll, D. L.; Park, Y. W. *Nano Lett*. **2003**, *3*, 839−842.

10.1021/ja042554y CCC: $30.25

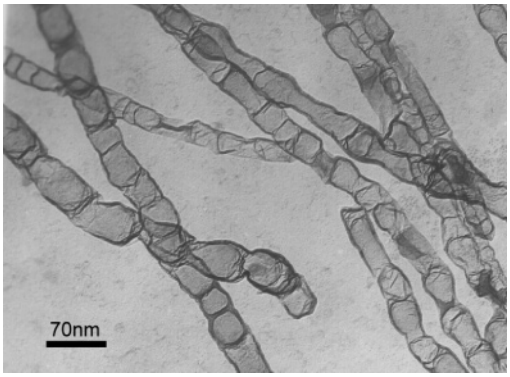

Figure 1. TEM image of the N-doped carbon nanotubes.

electronic defect states.[16] Electron-rich substitutions in sp^2-bonded graphene lattices could easily lead to "out of plan" bonding configurations, which may induce curvature and closure of the system during growth before tubular formation occurs.[14] Though many theoretical analysis and experiments have been devoted to the electronic and thermal properties of N-doped MWCNTs, there are, to the best of our knowledge, no reports concerning direct electronic transport measurements of an individual N-doped nanotube performed at room temperatures and below. In this article, we introduce nitrogen into the carbon nanotubes as donor states to the system and study the electronic properties of the N-doped MWCNTs at different temperatures.

Results and Disscusion

The N-doped MWCNTs (CN_x, $x \leq 0.09$) used in our experiments were prepared by chemical vapor deposition.[17] Transmission electron microscopy (TEM) observations show that the average outer diameter is about 50 nm (Figure 1). The nanotubes were dispersed in chloroform using ultrasonic agitation for 15 min. A drop of the solution was then spread onto a 500-nm-thick thermal oxidized silicon surface with Ti/Au pads that had already been prepared with the photolithography method. Pt leads connecting the CNTs to the Ti/Au pads were fabricated by a probe point extension Focused Ion Beam System (IDS P2X) using a $(CH_3C_5H_4)Pt(CH_3)_3$ carrier gas. Therefore, we can get a field-effect transistor (FET) device based on an individual N-doped carbon nanotube. The distance between two contacting points varied from ~2 to ~6 μm for the different patterns (Figure 2). The two terminal resistances was measured using Keithley 199 multimeter. The temperature-dependence measurements were carried out in a vacuum at temperatures ranging from 10 to 300 K. Electronic properties were measured using a probe station (Wentworth, MP1008) and a semiconductor parameter analyzer (HP 4140B).

Figure 3a shows a set of typical current versus source−drain voltage ($I-V_d$) curves obtained from an individual CN_x MWCNT FET at different gate voltages (V_g) in a vacuum. The conductivity of the nanotube increases with increasing positive V_g. The transfer properties of the CN_x NT FET have also been examined (Figure 3b). The current versus gate voltages ($I-V_g$) for a CN_x NT device recorded at different source−drain voltages are characteristic of an n-channel metal oxide semiconductor FET.

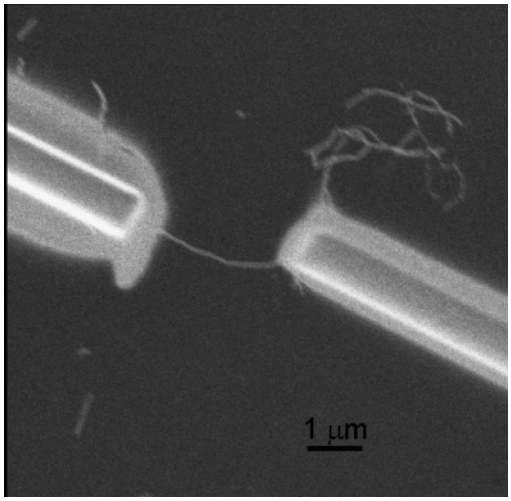

Figure 2. Scanning electron microscope image of an individual N-doped carbon nanotube device.

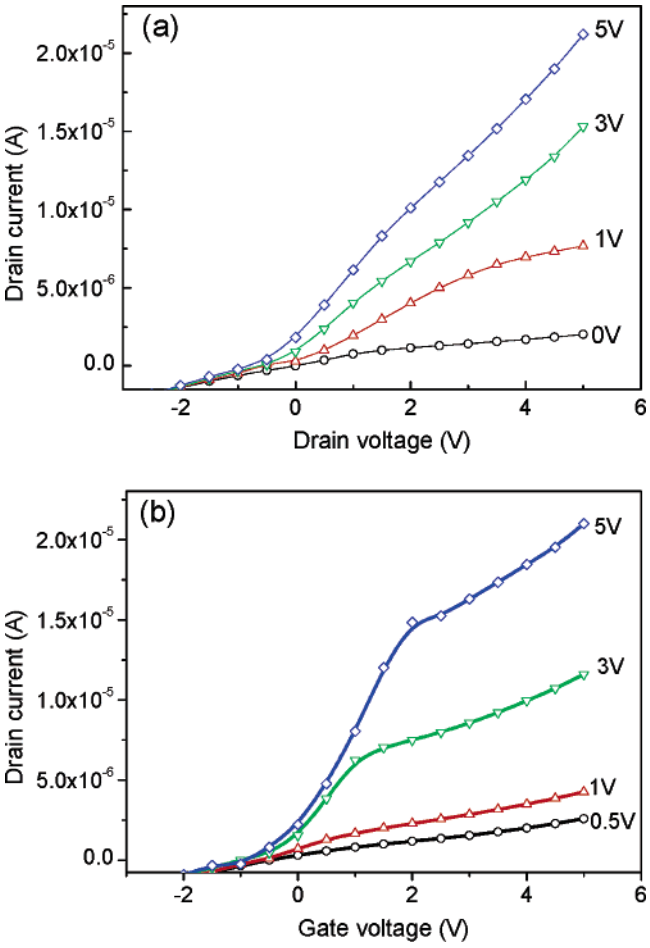

Figure 3. Output (a) and transfer (b) characteristics of an N-doped carbon nanotube FET in the vacuum.

We attribute this n-type behavior to the nitrogen-doping based on previous studies of nitrogen-doped materials. The threshold voltage necessary to completely deplete the nanotube is about −0.6 V at 5 V bias. The carrier concentration along the nanotube is estimated to be 1.4×10^6/cm according to ref 18. The mobility

(16) Crespi, V. H.; Cohen, M. L.; Rubio, A. *Phys. Rev. Lett.* **1997**, *79*, 2093−2096.
(17) Wang, X. B.; Liu, Y. Q.; Zhu, D. B.; Zhang, L.; Ma, H. Z.; Yao, N.; Zhang, B. L. *J. Phys. Chem. B* **2002**, *106*, 2186−2190.
(18) Martel, R.; Schmidt, T.; Shea, H. R.; Hertel, T.; Avouris, Ph. *Appl. Phys. Lett.* **1998**, *73*, 2447−2449.

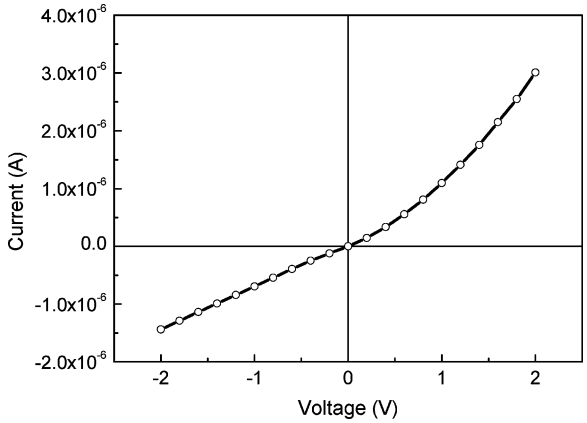

Figure 4. Current−voltage ($I-V$) characteristic of an N-doped carbon nanotube in a vacuum at room temperature.

of the carriers can be deduced to be 895 cm^2/Vs from the slope $dI/dV_g = \sim 4.5 \times 10^{-7}$ A/V at $V_d = 0.5$ V as determined from the linear portion of the $I-V_g$ curves. The mobility greatly exceeds the earlier one reported for semiconducting MWCNTs.[18] However, the on/off ratio is less than 100 due to structural and chemical defects. The electronic properties of N-doped carbon nanotubes, such as carrier density and mobility, will vary drastically depending on the doping level since the conductivity of undoped nanotube is dominated by the lattice. N doping can enter into the lattice of carbon nanotube and form the covalent bonding with C (N coordinated to three C atoms in a sp^2-like fashion) and change the lattice structure of nanotubes. The addition electrons will be injected into the structure, which induces higher carrier density in N-doped carbon nanotube. However, it will also introduce many chemical and structural defects while generating additional electron as a donor element. Therefore, the carrier density and mobility of nanotubes depend on the doping level, the number of N atoms, the number of removed C atoms within the hexagonal sheet, and the defects in the tube. The electronic properties of nanotube would be also affected by the diameter of NTs. If we want to observe the genuine quantum effects in doped CNTs, dopants must be present in NTs with small diameter (<1−2 nm). Thus far, many methods have been exploited to synthesize CN_x nanotubes, such as arc discharge method,[19] laser ablation,[20] chemical vapor deposition,[21] and pyrolysis.[22] Despite these efforts, the control over N content and diameter viability is still beyond reach.

To further understand the energy-band structure in the n-type CN_x NT FET, we investigated the contact condition between the tube and Pt electrodes. Figure 4 shows a plot of the typical current versus voltage curve of an individual N-doped nanotube in a vacuum condition. These devices typically exhibit nonlinear behavior, which might be induced by Fermi level pinning at the nanotube Pt electrode interface. When a tube contacts with Pt electrodes, a Schottky barrier will be formed due to the different work functions of the tube and Pt. To further explore the electronic properties of the CN_x nanotube device, we measured the $I-V$ curves as a function of temperature, as shown in Figure 5. A temperature dependence on the forward and reverse bias current was observed. An Arrhenius plot of the conductance is shown (inset), in which the thermionic and tunneling contributions could be identified.[23] The tunneling current dominated at low temperatures. A clear thermionic regime was observed in carrier transport at temperatures above $T = 130$ K (Figure 5 inset). Determination of the barrier height (ϕ_b) and barrier width (d_b) is essential in understanding the electronic transport properties through the Schottky barrier junction (SBJ). The $I-V$ characteristics of devices often deviate from ideal SBJ behavior. In this case, the generalized diode equation can be applied:[24]

$$I = I_{sat}[\exp(qV/nkT) - 1] \quad (1)$$

where q is the electronic charge, V is the voltage across the junction, I_{sat} is the reverse bias saturation current, and n is known

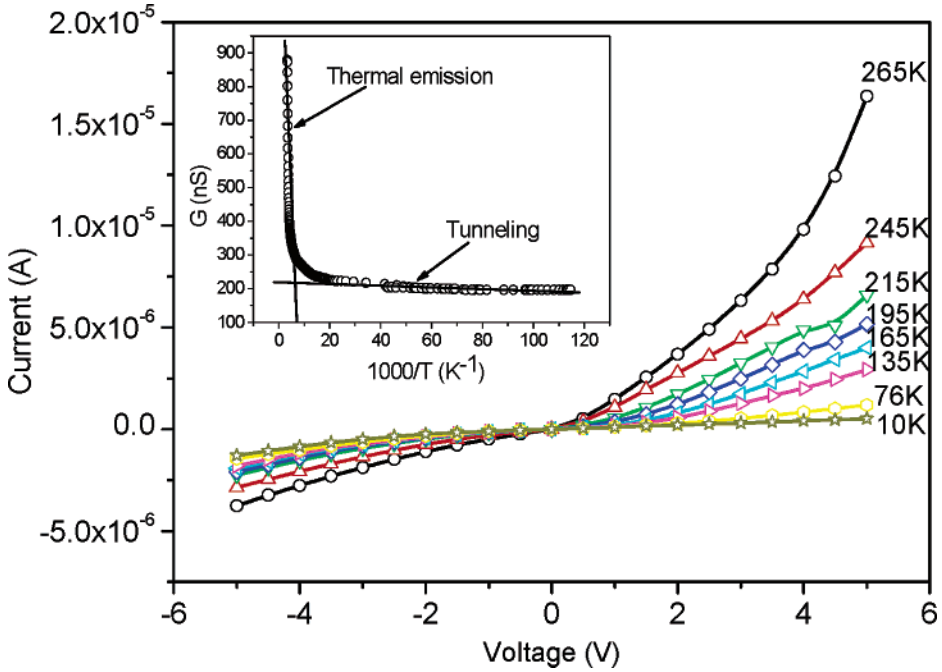

Figure 5. Current voltage characteristics of an N-doped carbon nanotube in a vacuum at different temperatures. Inset: Arrhenius plot of electronic transport in a vacuum.

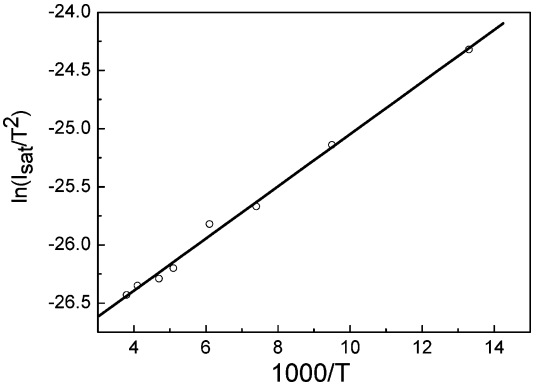

Figure 6. Extraction of the Schottky barrier height by a linear fit of the $\ln(I_{sat}/T^2)$ versus $1/T$ plot. The slope of the linear fit is used to determine the barrier height, and the intercept on the I_{sat}/T^2 axis gives the value of A.

as the ideality factor. I_{sat} is given by[24]

$$I_{sat} = SAT^2 \exp(-q\phi_b/kT) \quad (2)$$

where S is the diode area, A is the Richardson constant, and ϕ_b is the effective barrier height of the junction. Using eq 2, we constructed a plot of $\ln(I_{sat}/T^2)$ versus $1/T$ (Figure 6).

The slope of the plotted data was used to extract ϕ_b, yielding an average value of $\phi_b = 0.2$ eV. The barrier width, d_b, can be estimated using $d_b = \sqrt{2\epsilon\epsilon_0/eN_A(W_{Pt} - W_{CNT} - k_BT/e)}$,[25] where N_A is the electron concentration that can be estimated to be equal to the electron density in the tube, N_e. Electron density is calculated as $N_e = C_g V_g^t/eL$ when $C_g = 2\pi\epsilon\epsilon_0 L/\ln(h/d)$,[18] C_g is the capacitance of the tube with respect to the gate, V_g^t is the gate voltage required to deplete holes in the tubes, ϵ is the average dielectric constant of the transistor, and h is the thickness of the insulating layer between the tube and the gate. For the CNT FET studied here, V_g^t is determined to be ~ -0.6 V using the assumption that electrons are sufficiently depleted. Using $W_{Pt} = 5.7$ eV,[26] $W_{CNT} = 4.5$ eV,[26] $\epsilon = 2.5$,[18] $h = 500$ nm, and $L = 3$ μm, we estimate d_b and N_e to be $\sim$50 nm and $\sim 1.4 \times 10^6$/cm, respectively. A large d_b indicates that the barrier width cannot be neglected compared with the tube length between the drain and source. Therefore, the energy band in the tubes should be bent between the drain and source when no gate voltage and drain−source bias are applied.[25] This is contrary to the semiclassical band-bending model.[26] On the basis of the above analysis, the band structure of a tube transistor is determined and presented in Figure 7, in which the energy band of the tube becomes bent along the tube and where the Fermi level E_F lies below the conduction band edge of the tube due to the Fermi level pinning by the metal electrodes.

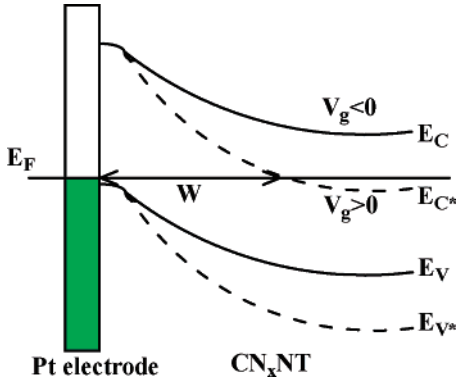

Figure 7. Schematic energy band diagram in the region of the junction between an N-doped carbon nanotube and the electrodes at different gate biases. W denotes the barrier thickness for electron injection. E_c, E_c^* and E_V, E_V^* represent the conduction and valence band energy of nanotube, respectively. * denotes the effects of gate bias.

The Schottky barrier height and width of the Pt electrode and the tube are greatly influenced by the gate voltage, because the tube is coupled from the drain and source. By sweeping V_g, the energy band of the tube can be moved up and down. According to the Derycke and Avouris model,[27,28] carrier transport in the CNT FET is determined by tunneling through the metal-semiconductor Schottky barrier. The electrostatic field of the gate can strongly modulate the effective barrier height and thickness of the metal and CN_x nanotube interface. In the presence of negative gate bias, no current passes through the higher and thicker Schottky barrier. With positive gate bias, however, the band bends strongly downward and the barrier becomes increasingly thinner because of the increased screening. Hence, the electrons can tunnel easily through the barrier. As a result, the devices show n-type characteristics FET.

Conclusions

In conclusion, field-effect transistors were fabricated using an individual multiwalled N-doped carbon nanotube. The transistors showed a clear n-type behavior and high mobility (895 cm^2/Vs). The Schottky barrier is formed between the nanotubes and Pt electrodes. The barrier height and barrier width are about 0.2 eV and 50 nm, respectively. Temperature dependence of two-terminal transport experiments suggested that transport was dominated by thermionic emission and tunneling process over 0.2 eV Schottky contact barrier. As a result, CNTs doped with N exhibit novel electronic properties that are not found in their pure carbon counterparts. Therefore, the N-doped carbon nanotubes would be extremely useful in the development of field-emission sources, nanoelectronics, sensors, and composite materials in the future.

Acknowledgment. We gratefully acknowledge financial support from the National Natural Science Foundation of China (NSFC), the Major State Basic Research Development Program, and the Chinese Academy of Sciences.

JA042554Y

(19) Glerup, M.; Steinmetz, J.; Samaille, D.; Stephan, O.; Enouz, S.; Loiseau, A.; Roth, S.; Bernier, P. *Chem. Phys. Lett.* **2004**, *387*, 193−197.
(20) Zhang, Y.; Gu, H.; Suenaga, K.; Iijima, S. *Chem. Phys. Lett.* **1997**, *279*, 264−267.
(21) Terrones, M.; Hsu, W. K.; Terrones, H.; Zhang, J. P.; Ramos, S.; Hare, J. P.; Castillo, R.; Prassides, K.; Cheetham, A. K.; Kroto, H. W.; Walton, D. R. M. *Chem. Phys. Lett.* **1996**, *259*, 568−573.
(22) Terrones, M.; Grobert, N.; Olivares, J.; Zhang, J. P.; Terrones, H.; Kordatos, K.; Hsu, W. K.; Hare, J. P.; Townsend, P. D.; Prassides, K.; Cheetham, A. K.; Kroto, H. W.; Walton, D. R. M. *Nature* **1997**, *388*, 52−55.
(23) Martel, R.; Derycke, V.; Lavoie, C.; Appenzeller, J.; Chan, K. K.; Tersoff, J.; Avouris, Ph. *Phys. Rev. Lett.* **2001**, *87*, 256805−1−256805−4.
(24) Sharma, B. L. *Metal-Semiconductor Schottky Barrier Junctions and Their Applications*; Plenum Press: New York, 1984.
(25) Liu, K.; Burghard, M.; Roth, S. *Appl. Phys. Lett.* **1999**, *75*, 2494−2496.
(26) Tans, S. J.; Verschueren, A. R. M.; Dekker, C. *Nature (London)* **1998**, *393*, 49−51.
(27) Appenzeller, J.; Knoch, J.; Derycke, V.; Martel, R.; Wind, S.; Avouris, Ph. *Phys. Rev. Lett.* **2002**, *89*, 126801−1−126801−4.
(28) Derycke, V.; Martel, R.; Appenzeller, J.; Avouris, Ph. *Appl. Phys. Lett.* **2002**, *80*, 2773−2775.